*Brain* (2000), **123,** 1471–1480

# Correlation of MRI lesions with visual psychophysical deficit in secondary progressive multiple sclerosis

P. A. Caruana,[1,2] M. B. Davies,[1,2] S. J. M. Weatherby,[1,2] R. Williams,[3] N. Haq,[3] D. H. Foster[4,5] and C. P. Hawkins[1,2]

*Keele Multiple Sclerosis Research Group: [1]Department of Neurology, Royal Infirmary, [2]Keele University School of Post-Graduate Medicine, [3]Cornwall House Magnetic Resonance Imaging Centre and [4]Department of Communication and Neuroscience, Keele University, Stoke-on-Trent and [5]Visual and Computational Neuroscience Group, Department of Optometry and Neuroscience, University of Manchester Institute of Science and Technology, Manchester, UK*

*Correspondence to: Dr Brendan Davies, Department of Neurology, North Staffs Royal Infirmary, Princes Road, Stoke-on-Trent ST4 7LN, UK*
*E-mail: Brendand@mcmail.com*

## Summary

**The aim of this work was, first, to clarify the nature of the relationship between the sensory deficit in the demyelinated visual pathway and morphological changes revealed by MRI and, secondly, to test whether there was a preferential effect of demyelination for either the magnocellular or parvocellular pathway in established multiple sclerosis. Twenty-four patients with secondary progressive multiple sclerosis were studied psychophysically and by MRI of the optic nerve and brain. MRI was performed with a Phillips (0.5T) scanner. Visual pathway MRI lesion load was evaluated independently using the total optic nerve lesion length and lesion area seen on STIR (short inversion time inversion recovery) images of the optic nerve and the total post-chiasmal lesion area on $T_1$-, $T_2$- and proton-density-weighted images of the brain. Psychophysical tests determined 75%-seeing thresholds for horizontal gratings consisting of isoluminant red and green sinusoids of the same spatial frequency combined out-of-phase for preferential stimulation of the parvocellular system and in-phase for preferential stimulation of the magnocellular system. It was found that, in this group of patients, visual psychophysical loss was significantly correlated with lesion area seen on proton density MRI sequences of the post-chiasmal visual pathway, and that the parvocellular pathway was more affected than the magnocellular pathway, especially at lower spatial frequencies.**

**Keywords**: multiple sclerosis; MRI; visual psychophysics; magnocellular/ parvocellular; chromatic

**Abbreviations**: EDSS = Kurtzke Expanded Disability Status Score; FOV = field of view; PEST = parameter estimation by sequential testing; STIR = short inversion time inversion recovery

## Introduction

The visual pathway is one of the most commonly affected sites in multiple sclerosis (McDonald and Barnes, 1992). A spectrum of pathology exists, ranging from acute optic neuritis with relatively sudden loss of vision to subtle subclinical disturbance evident only on neurophysiological or psychophysical testing. The relationship between functional disturbance of the visual system and structural abnormality in established multiple sclerosis is unclear.

At present, MRI is the optimum technique for the identification of multifocal white matter lesions in the brain in multiple sclerosis *in vivo* (Young *et al.*, 1981; Ormerod *et al.*, 1987; Miller, 1997). Such lesions are thought to represent plaques of inflammation, demyelination, oedema or gliosis (Ormerod *et al.*, 1986, 1987; Hawkins *et al.*, 1990). Additionally, MRI has been used in optic neuritis and multiple sclerosis to identify abnormalities in the optic nerve (Miller *et al.*, 1988; Barkhof *et al.*, 1991; Youl *et al.*, 1991; Davies *et al.*, 1998) and post-chiasmal visual pathway (Hornabrook *et al.*, 1992; Plant *et al.*, 1992).

Involvement of the visual system in multiple sclerosis was

noted as early as 1890 by Uhthoff and subsequently in large case series (Poser *et al*., 1979; Perkin and Rose, 1979). Abnormality of the visual evoked response (Halliday *et al.*, 1973) and histological study of the optic nerve and post-chiasmal pathway (Ulrich and Groebke-Lorenz, 1983) have also identified visual pathway pathology. Studies in acute optic neuritis using STIR (short inversion time inversion recovery) images with gadolinium-DTPA enhancement have suggested that blood–brain barrier breakdown associated with inflammation is the predominant cause of functional deficit (Youl *et al.*, 1991). Treatment with steroids did not appear to influence visual outcome or lesion length measured on optic nerve STIR images (Beck and Cleary, 1993; Kapoor *et al.*, 1998).

Visual psychophysics offers an established, sensitive approach to detecting and measuring disturbance in the different modalities of vision, the results of which may be interpreted in terms of the underlying anatomy and physiology. Anatomical studies show a division of the anterior human visual system into magnocellular and parvocellular pathways (Shapley, 1990). The magnocellular pathway contains ~10% of optic nerve fibres (Silveira and Perry, 1991) and is involved in the detection of achromatic stimuli of low-to-medium spatial frequency. The parvocellular pathway contains ~80% of optic nerve fibres and is involved in the detection of chromatic stimuli of low-to-medium spatial frequency and achromatic stimuli of high spatial frequency (Ingling *et al.*, 1983; Merigan *et al.*, 1991). The parvocellular pathway is thought to provide the substrate for opponent signals from red- and green-sensitive cones. [A third pathway, the koniocellular pathway (Casagrande, 1994), may provide the substrate for signals from blue-sensitive cones.] The temporal responses of the magnocellular and parvocellular pathways differ: the magnocellular pathway is more sensitive at high temporal frequencies and the parvocellular pathway at low temporal frequencies. The difference in temporal response may, however, be partly confounded by the general effects of demyelination, in that if demyelination acts simply as a low-pass filter, then all high-frequency responses will be attenuated independently of fibre type (Mason *et al.*, 1982; Plant and Hess, 1985; Snelgar *et al.*, 1985; Herbst *et al.*, 1997; Vleugels *et al*., 1998). Although initially well defined, there are conflicting reports as to whether the pathways remain segregated cortically (DeYoe and Van Essen, 1988; Maunsell *et al.*, 1990, 1999; Baizer *et al.*, 1991; Regan *et al.*, 1991; Ferrera *et al.*, 1992; Nealey and Maunsell, 1994).

MRI is used currently as a putative surrogate marker of pathophysiological change in multiple sclerosis. A recent study in established multiple sclerosis has shown a correlation between optic nerve lesion load on MRI and abnormality of the visual evoked potential (Davies *et al*., 1998). Morphological change in the visual pathway on MRI may thus prove useful in interpreting other measures of visual dysfunction. Twenty-four patients with secondary progressive multiple sclerosis were therefore studied by visual psychophysics and by MRI of the optic nerve and brain to compare functional deficit with structural abnormality in the visual system.

## Methods

### *Patients and controls*

The study was approved by the ethical committee of the North Staffordshire Hospital and informed consent was obtained from all subjects. Patients included in the study had clinically definite secondary progressive multiple sclerosis of at least 2 years duration as defined by the Poser criteria (Poser *et al*., 1983). Patients were aged 18–55 years and had a Kurtzke Expanded Disability Status Score (EDSS) of 2.5–6.0 and no past history of serious eye disease or diabetes mellitus. There was no history of steroid treatment or other immunotherapy in the 2 months before the study.

The study included seven male and 17 female patients with a mean age of 40.5 years (range 24–53 years), mean disease duration of 11 years (range 3–24 years) and a mean Kurtzke EDSS score of 5.0. Five patients (eight eyes) had a previous history of acute unilateral optic neuritis in the course of their illness. The mean duration since the last attack of optic neuritis was 11.9 years (range 4–23 years). Twenty-three healthy age- and sex-matched volunteers were also studied to provide a control population for visual psychophysics.

### *Ophthalmic examination*

Snellen acuity was obtained for each eye at 6 m in standard lighting. Visual fields were obtained for each eye in all patients by clinical confrontation and centrally using a Bjerrum screen. Colour vision was tested monocularly with Ishihara pseudoisochromatic plates, and pupil reactions were also tested. Full slit-lamp examination was performed to exclude corneal, lenticular and media opacities. The fundus was examined using direct and indirect fundoscopy.

Snellen acuity was 6/9 or better in 45 out of 48 eyes (93%), and it was 6/9 or better in the eight eyes with previous acute optic neuritis. Visual field testing demonstrated small arcuate scotomata in 16 out of 48 eyes (33%) in a pattern that has been described previously (Patterson and Heron, 1980). Scotomata were all outside the central 15° of central vision. Only two out of these 16 eyes had a previous history of acute optic neuritis. Colour vision was mildly impaired in seven out of 48 eyes (15%; 3–4 Ishihara plates incorrect out of 21); moderately impaired in two out of 48 eyes (4%; 5–10 plates incorrect out of 21) and severely impaired in one eye (>10 plates incorrect). Colour vision was abnormal in five out of eight eyes with previous optic neuritis. A relative afferent pupillary defect was not seen in any of the 48 eyes and optic disc pallor was apparent in only four out of 48 eyes.

### *MRI and visual pathway lesion analysis*

A Phillips 0.5 Tesla Gyroscan was used for all imaging. The patient's head was positioned comfortably in a head holder

to minimize movement. A sagittal pilot scan was performed (TR 300–500 ms, 128 matrix excitation) with the inter-hemispheric fissure used as the initial landmark. Positioning of the patient was corrected for ear-to-shoulder tilt in the coronal sections and right-to-left rotation on axial sections. Optic nerve imaging used a coronal STIR sequence (IR 1400/140/25) to identify lesions within the optic nerve. The STIR sequence consisted of 12 contiguous 4 mm slices with a 1 mm interslice gap, a field of view (FOV) of 20 cm, with two acquisitions, obtained sequentially anterior to posterior from the optic nerve papilla to the optic chiasm.

Imaging of the post-chiasmal pathway used axial $T_1$-weighted (SE 550/10), conventional $T_2$-weighted (SE 2760/80) and proton-density-weighted (SE 2760/20) brain images to show the post-chiasmal pathway from the optic tract anteriorly to the visual cortex posteriorly. These images were obtained as contiguous axial 5 mm slices with an interslice gap of 0.5 mm and FOV of 23 cm. Two acquisitions were used for the $T_1$-weighted sequences and one acquisition for the variable echo sequences. The post chiasmal pathway was identified by a neuroradiologist (N.H.) on relevant axial brain images for each sequence using recognized landmarks (Miller, 1982) and subsequently divided anatomically into the optic tracts, the lateral geniculate nuclei, the optic radiations and the projections to the primary visual cortex.

Subsequently, a neuroradiologist (N.H.) and MRI research fellow (M.B.D.) independently identified lesions within the visual pathway on MRI unaware of the patient's identity and history. Lesions involving the optic nerve or post-chiasmal pathway on MRI were only scored when agreed by both assessors and were marked on hardcopy before quantitative analysis.

Involvement of the optic nerve on coronal STIR images was defined as an abnormal focal area of high signal originating within the optic nerve (Fig. 1). Quantitative analysis of optic nerve involvement on STIR involved measurement of total optic nerve lesion area (total area of optic nerve high signal abnormality measured on coronal images). A computer-assisted manual outlining package was used (by M.B.D.) to outline the area of abnormal signal in each involved optic nerve on coronal images. These areas were then summed to give the total lesion area within that optic nerve. It was assumed that the high signal abnormality on STIR sequences was due to involved optic nerve rather than to cerebrospinal fluid in the optic nerve sheath. A small interslice gap was used and it was assumed that abnormality on adjacent slices traversed the interslice gap.

Because of limited image resolution, it was difficult to identify chiasmal lesions clearly on coronal optic nerve STIR images and on axial brain images, and, therefore, chiasmal involvement could not be assessed accurately in this study.

Involvement of the post-chiasmal pathway on MRI was defined on axial images as discrete areas of hypointensity on $T_1$-weighted images and discrete areas of high signal on $T_2$-weighted and proton-density-weighted images identified within the optic tract, the lateral geniculate nucleus, the optic radiations and the projections to the visual cortex (Fig. 2). A computer-assisted manual outlining package was used as before (by M.B.D.) to identify lesions within the post-chiasmal pathway on each sequence. Their areas were calculated and then summed to give the total post-chiasmal pathway lesion area.

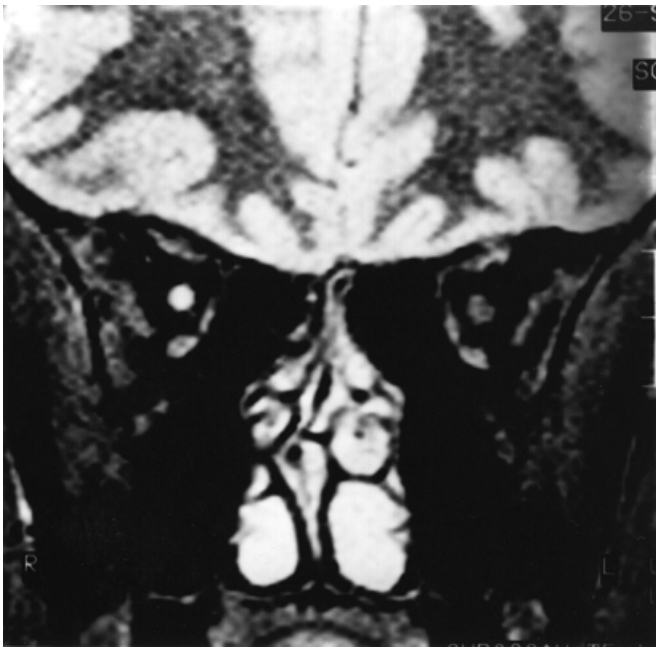

**Fig. 1** Focal area of high signal abnormality within the right optic nerve in a patient with secondary progressive multiple sclerosis and no past history of optic neuritis.

The intra-operator reproducibility of optic nerve STIR and post-chiasmal quantitative area measurement was assessed as part of the study. A single observer performed the initial analysis of the whole patient cohort (M.B.D.) and the same observer subsequently quantified the lesion area in 10 randomly selected patients more than a year later. Statistical analysis of intra-observer reproducibility was calculated using a previously described methodology (Filippi *et al*., 1995).

## *Psychophysics*

A visual stimulus in the form of a sinusoidal grating was presented on a 20 inch monitor (Sony, Japan; Trinitron). The stimulus was created with a raster-graphics generator (Cambridge Research Systems, UK; VSG, version 2/2, with Psycho software version 4.3), controlled by a laboratory computer. The grating appeared within a circular window of 8° visual angle, which produced at least four visible cycles of the coarsest gratings (0.25 cycles/degree). A graded annular diffuser placed over the stimulus region reduced any potential edge effects of the circular window. A black fixation cross of 0.5° visual angle was placed at the centre of the screen. Mean luminance of the screen was 20 cd/m$^2$. Stimuli were viewed monocularly at a distance of 82 cm. All photometric calibrations were performed at the viewing position.

The psychophysical tests produced 75%-seeing thresholds

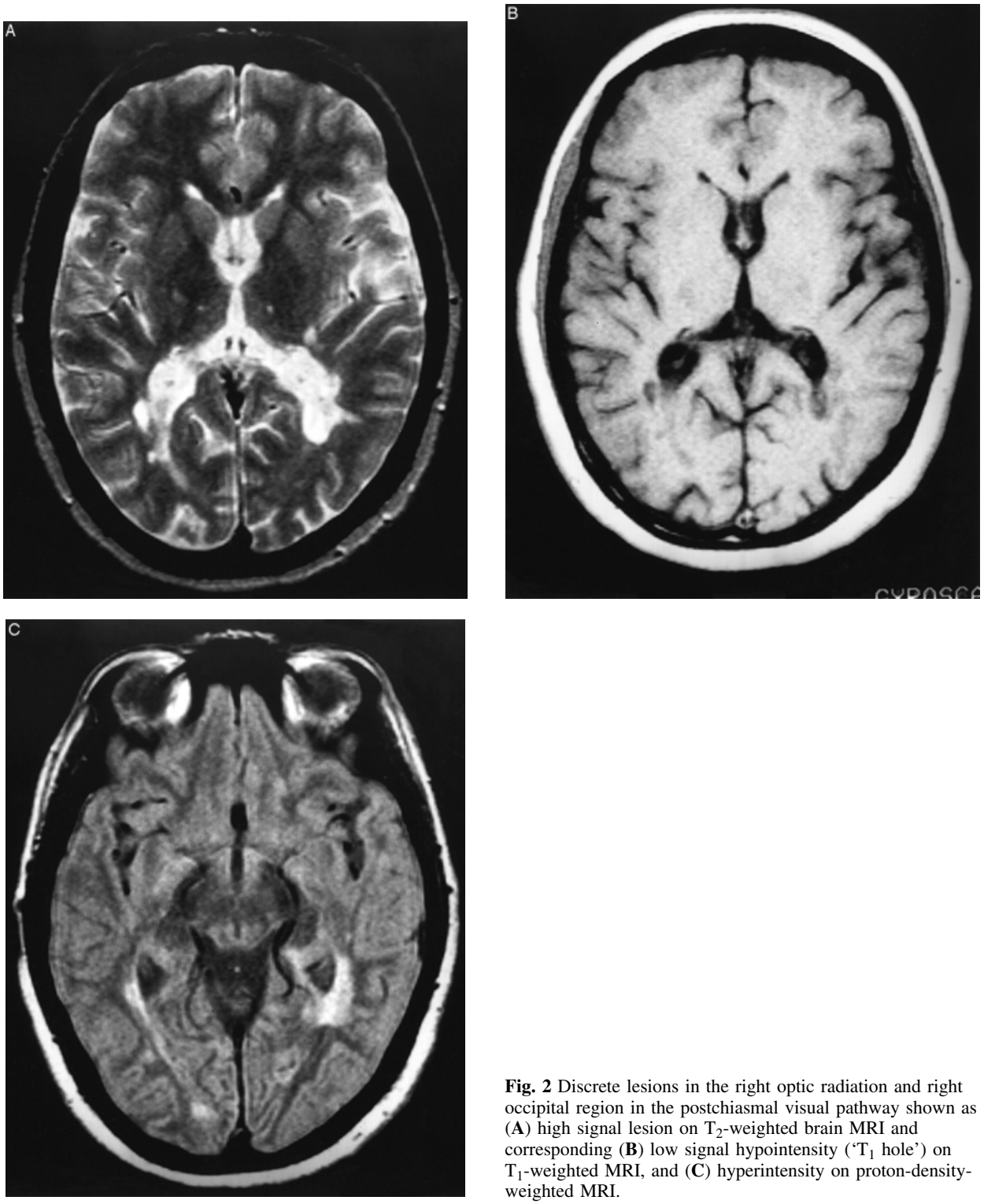


**Fig. 2** Discrete lesions in the right optic radiation and right occipital region in the postchiasmal visual pathway shown as (**A**) high signal lesion on $T_2$-weighted brain MRI and corresponding (**B**) low signal hypointensity ('$T_1$ hole') on $T_1$-weighted MRI, and (**C**) hyperintensity on proton-density-weighted MRI.

for contrast sensitivity by means of an adaptive routine (parameter estimation by sequential testing, PEST; Taylor and Creelman, 1967) for left and right eyes examined in random order. The horizontal, sinusoidally modulated gratings had spatial frequencies of 0.25, 1.0 and 4.0 cycles/degree. Although this was not an investigation into temporal responsiveness, the gratings were made to drift slowly upwards in order to minimize the effects of local spatial adaptation to the stimuli. Each grating moved at the same low speed of 0.4 degrees/s (so that if there were a cue to inadvertent eye tracking it would be the same for each condition). The corresponding temporal frequencies of the gratings (0.1, 0.4 and 1.6 cycles/s, respectively) were about an order of magnitude below those at which any temporal

effects of demyelination might be expected to occur. Subjects gazed steadily at the fixation target during stimulus presentation. To provide a starting point for the PEST routine, an initial approximate threshold was obtained for each grating by a method of adjustment. Stimulus duration was 1.0 s with a 0.3 s rise, 0.4 s plateau and 0.3 s fall. The luminances of the red and green components in the isoluminant gratings were estimated by a method for non-flickering stimuli similar to that described by Mullen (Mullen, 1985). Thus gratings of all three spatial frequencies were shown three times, comprising mixtures: 25% red / 75% green; 50% red / 50% green; and 75% red / 25% green. The resulting nine possible stimuli were presented in random order to each eye. A simple quadratic formula was used to compute the optimum red/green mixture for isoluminance at each spatial frequency.

The PEST routines were then started. The red and green components were presented 180° out-of-phase (giving the appearance of alternating red and green bands, effectively high chromatic modulation with no luminance modulation) for preferential stimulation of the parvocellular system; and in-phase (giving the appearance of bright yellow bars alternating with dark yellow bars, effectively high luminance modulation with no chromatic modulation) for preferential stimulation of the magnocellular system. These six conditions were presented in a random order for each eye tested. The whole series of measurements required 60–75 min depending on the patient's speed in learning the task and need for rest. Data were analysed offline to yield a contrast threshold and standard deviation estimated by a bootstrap procedure (Foster and Bischof, 1991) for each spatial frequency and phase arrangement of red and green gratings. Weighted mean thresholds were calculated for each spatial frequency and phase arrangement for patients and controls.

Psychophysical data were sorted into two groups (left and right eyes) to avoid introducing spurious correlations from the eyes of the same patient (Glynn and Rosner, 1992).

### *Psychophysical–MRI correlation*

Psychophysical data were combined to give a mean magnocellular threshold and a mean parvocellular threshold for each eye. The mean total optic nerve lesion length and the mean total post-chiasmal lesion area were calculated for patients with normal and with abnormal psychophysical thresholds. Robust Pearson product–moment correlation coefficients (trim value 0.05) were calculated with percentiles estimated by the bias-corrected and adjusted (BCa) bootstrap method (Efron and Tibshirani, 1993). Where comparisons were made involving multiple measures, Bonferroni corrections were applied to reported *P*-values.

## Results

### *MRI*

#### *Optic nerve (coronal STIR images)*

Nineteen out of 24 patients (79%) had abnormal optic nerve STIR images with 28 out of 48 optic nerves (58%) studied showing intrinsic high signal abnormality. Nine patients (38%) had bilateral optic nerve lesions. The mean total optic nerve lesion area was 7.43 $mm^2$ (range 0–31.7 $mm^2$) for the right eye and 7.88 $mm^2$ (range 0–37.1 $mm^2$) for the left eye.

#### *Post-chiasmal visual pathway (axial $T_1$-, $T_2$- and proton-density-weighted images)*

Fifteen out of 24 patients (63%) had $T_1$ hypointensities in the post-chiasmal pathway. Five patients (21%) had bilateral lesions. The mean total lesion area was 33.5 $mm^2$ with range 0–136 $mm^2$. Twenty out of 24 patients (83%) had post-chiasmal pathway lesions, with bilateral lesions in 83% of these patients. The mean total lesion area was 181.8 $mm^2$ (range 0–1634 $mm^2$). Twenty-one out of 24 patients (88%) had post-chiasmal pathway lesions, with bilateral lesions in 88% of these patients. The mean lesion area was 278.7 $mm^2$ (range 0–2660 $mm^2$). There was no significant difference in the quantitative post-chiasmal MRI lesion area in patients with and without a past history of optic neuritis for any sequence.

The reproducibility of quantitative lesion area analysis on STIR, $T_1$-, $T_2$- and proton-density-weighted images produced median intra-observer agreement values of 97% (range 76–100%), 90% (range 56–97%), 88% (range 28–98%) and 85% (range 4–99%), respectively using a manual outlining technique.

### *Psychophysical thresholds*

The normal range for psychophysical thresholds was taken as the weighted means for control subjects $\pm 2$ weighted standard errors of the weighted mean. As a preliminary test, mean weighted thresholds were compared for patients with and without a past history of optic neuritis. There was no significant difference and all patients were included in the study.

Every eye had at least one threshold higher than the normal range. In 14 patients (58%), all six psychophysical thresholds were higher than the normal range in both eyes. There were more abnormal thresholds for the parvocellular pathway than for the magnocellular pathway (right eyes $P < 0.05$; left eyes $P < 0.01$). Figure 3 shows weighted mean thresholds for patients and normal controls for stimuli preferential for parvocellular (Fig. 3A) and magnocellular (Fig. 3B) pathways. In terms of the proportional increase in thresholds for patients with respect to those for normal controls, the deficit was greater for the parvocellular pathway than for the magnocellular pathway, particularly at lower spatial frequency (see Table 1). There was a significant correlation in psychophysical loss between the two eyes ($r = 0.83$, $P < 0.01$).

### *The relationship between MRI lesion load and psychophysical thresholds*

The mean total lesion area on all post-chiasmal MRI sequences of the visual pathway was greater in patients

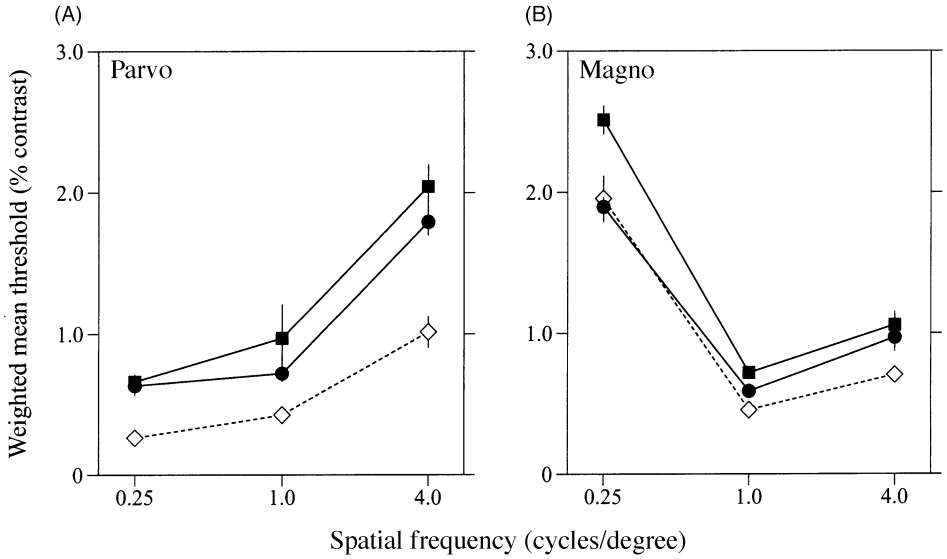


**Fig. 3** Weighted mean thresholds ±1 weighted standard error in patients with secondary progressive multiple sclerosis and in normal control subjects. Stimuli preferential for (**A**) parvocellular and (**B**) magnocellular pathways. Data for 24 patients and 23 controls. Filled squares = patient's right eye; filled circles = patient's left eye; open diamonds = normal controls.

**Table 1** *Loss in contrast sensitivity for patients in comparison with normal controls*

| Spatial frequency (cycles/degree) | Percentage increase in threshold | | | |
|---|---|---|---|---|
| | Parvocellular pathway | | Magnocellular pathway | |
| | Right eye | Left eye | Right eye | Left eye |
| 0.25 | 96.74 | 87.12 | 10.31 | –16.46 |
| 1.0 | 92.66 | 43.44 | 43.6 | 14.64 |
| 4.0 | 65.73 | 45.75 | 44.9 | 32.33 |

Percentage increase in psychophysical contrast thresholds in each eye for stimuli preferential for parvocellular and magnocellular pathways. Data for 24 patients and 23 controls.

whose psychophysical thresholds fell outside the normal range (Fig. 4). There was a significant correlation between the mean psychophysical threshold and the total post-chiasmal lesion area with proton-density-weighted images, for both magnocellular and parvocellular pathways, the Pearson product–moment correlation coefficients ranging from ~0.6 to 0.8 (see Table 2). There was no significant correlation with $T_1$- and $T_2$-weighted images, nor with STIR images of the optic nerve.

## Discussion

A quantitative analysis of the relationship between functional deficit and structural abnormality in established multiple sclerosis has not been reported previously. This study has revealed a strong correlation between visual psychophysical deficit and total post-chiasmal lesion area on proton density-weighted MRI, suggesting that morphological change in the post-chiasmal pathway has functional consequences. There was no reliable correlation between psychophysical deficit and lesion area on $T_1$- or $T_2$-weighted post-chiasmal MRI or for optic nerve STIR images.

Conventional MRIs are not specific for a particular type of histopathological lesion and any one MRI lesion may be heterogeneous. It is possible that proton-density images, by reflecting both an intracellular excess of water (inflammatory cells and gliosis) and expansion of the extracellular space (tissue oedema and water occupying the space created by loss of myelin and axons), are more representative of the range of pathologies affecting conduction of nerve impulses. In comparison, $T_2$-weighted images are more sensitive to extracellular water and therefore vasogenic oedema, demyelination or axonal loss, and may bias against a linear relationship with cumulative lesion load (Barnes *et al.*, 1987). However, neither sequence is specific pathologically, and it is still not possible to distinguish on proton-density-weighted images the main pathological substrates of the deficit in multiple sclerosis, namely demyelination and axonal loss. These considerations are necessarily speculative, and it may be simply that total lesion extent is the dominant factor. For example, $T_1$-hypointensities seen on $T_1$-weighted imaging have been shown to indicate tissue disruption and axonal loss and to correlate significantly with clinical disability when compared with conventional imaging (van Walderveen *et al.*, 1995, 1998). The close-to-zero correlation between psychophysical deficit and the area of post-chiasmal $T_1$-hypointensity may here reflect the fact that the area of lesion $T_1$-hypointensity in the visual pathway was small and therefore probably involved only a small proportion of the fibres in the posterior visual pathways. The strong correlation between post-chiasmal proton-density-weighted MRI abnormality and psychophysical deficit could also be due to the extent of the pathology being measured more sensitively

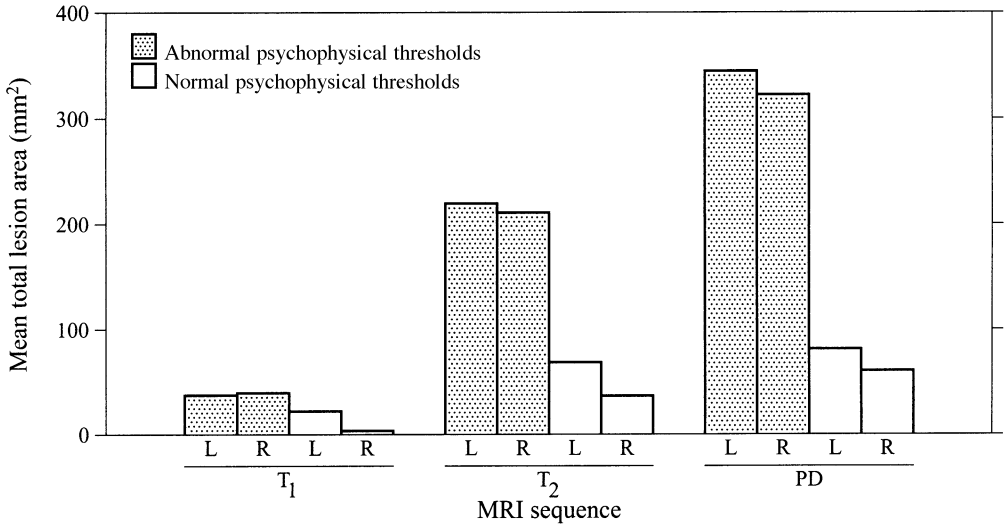


**Fig. 4** Mean total post-chiasmal lesion area ($mm^2$) on MRI in patients with abnormal and with normal psychophysical thresholds. Data for 24 patients.

**Table 2** *Correlation between psychophysical thresholds and total optic nerve (ON) STIR area and total postchiasmal pathway lesion area from $T_1$-, $T_2$- and proton density-weighted images*

| MRI lesion area | Parvocellular pathway | | | | Magnocellular pathway | | | |
|---|---|---|---|---|---|---|---|---|
| | Right eye | | Left eye | | Right eye | | Left eye | |
| | *r* | *P*-value | *r* | *P*-value | *r* | *P*-value | *r* | *P*-value |
| STIR ON | –0.11 | NS | 0.17 | NS | –0.19 | NS | 0.22 | NS |
| $T_1$ | 0.39 | <0.3 | 0.03 | NS | 0.15 | NS | 0.25 | NS |
| $T_2$ | 0.23 | NS | 0.09 | NS | 0.31 | <0.1 | 0.28 | NS |
| Proton density | 0.80 | <0.01 | 0.59 | <0.3 | 0.73 | <0.01 | 0.72 | <0.05 |

Thresholds were obtained for stimuli preferential for parvocellular and magnocellular pathways. Pearson product–moment correlation coefficients (*r*) are shown with *P*-values after Bonferroni correction for multiple comparisons ('NS' indicates $P \geqslant 0.3$). Data for 24 patients.

with proton-density-weighted images than with $T_2$- or $T_1$-weighted images, albeit with limited specificity. A recent study evaluating several MRI parameters also showed a strong correlation between lesion load on proton-density-weighted MRI and disability (Grimaud *et al.*, 1999), supporting the notion that proton-density-weighted images may be better than other commonly used sequences in measuring the extent of functionally important pathology. Compared with $T_2$-weighted imaging, proton-density-weighted sequences improve identification of multiple sclerosis lesions within the post-chiasmal visual pathway especially in the periventricular areas where lesions commonly affect the optic radiations.

This study used STIR imaging, which has now been superseded by fat-suppressed fast spin-echo sequences for better identification of lesions within the optic nerve and chiasm (Gass *et al.*, 1996). Lesion identification in the optic chiasm proved difficult here with the STIR sequence and possibly underestimated any contribution of the optic nerve to the psychophysical deficit. Nevertheless, the data suggest that a clinical attack of optic neuritis is not a prerequisite for the development of optic nerve lesions on STIR images.

There have been previous studies of the effects of multiple sclerosis and optic neuritis on the parvocellular and magnocellular visual pathways, with conflicting results. Several studies have suggested that luminance or magnocellular function was the more affected in optic neuritis and multiple sclerosis (Zisman *et al.*, 1978; Regan *et al.*, 1991; Phillips *et al.*, 1994), whereas others have suggested that chromatic or parvocellular function was the more affected (Fallowfield and Krauskopf, 1984; Mullen and Plant, 1986; Wall, 1990; Porciatti and Sartucci, 1996). A further group of studies has found luminance and chromatic function to be affected unselectively (Mason *et al.*, 1982; Foster *et al.*, 1983, 1985; Travis and Thompson, 1989; Dain *et al.*, 1990; Russell *et al.*, 1991; Schiller *et al.*, 1991; Vleugels *et al.*, 1998).

In the group of patients with secondary progressive multiple sclerosis examined here, the functional deficit for the parvocellular pathway was found to be greater than for the magnocellular pathway. A recent smaller study of 14 patients

with multiple sclerosis, all with a history of optic neuritis, indicated a similar higher vulnerability of the parvocellular pathway (Porciatti and Sartucci, 1996). In that study, chromatic and luminance function was assessed with visual psychophysics, and measurement of visual evoked potentials and pattern electroretinograms. The results of the present larger study, predominantly in patients without a past history of optic neuritis, are in accordance with these findings and further quantify the visual loss. It is possible that the parvocellular pathway is involved preferentially in established multiple sclerosis because parvocellular axons are smaller than magnocellular axons, and may, therefore, be more susceptible to the effects of mechanical or metabolic insult. The issue is complex, however, and the relative magnitudes of observed losses in luminance and chromatic function may depend on several factors including the size and position of the visual stimuli, their temporal characteristics, the luminance level at which the test takes place and the particular method used for determining isoluminance. Thus, small-field stimuli may show more specific responses from affected fibres but lead to difficulties in interpretation as the variation in the effect of demyelination may be confounded with the normal variation in fibre distribution within the retina (Plant and Hess, 1987). These and related problems in assessing the visual psychophysical deficit in optic neuritis and multiple sclerosis have been reviewed (Foster, 1986; Plant, 1991).

To summarize, the principal results of this study of established multiple sclerosis are, first, that there appears to be a strong correlation between quantitative area measurement on proton-density-weighted MRI and the functional deficit assessed psychophysically and, secondly, that the parvocellular pathway seems more affected than the magnocellular pathway, especially at lower spatial frequencies.

## Acknowledgements

We wish to thank Mr R. Knapper, Department of Communication and Neuroscience, Keele University, and Mrs Anne Bradley, Cornwall House MRI Centre, for technical assistance, and the Multiple Sclerosis Society of Great Britain and Northern Ireland for support.

### References

Baizer JS, Ungerleider LG, Desimone R. Organization of visual inputs to the inferior temporal and posterior parietal cortex in macaques. J Neurosci 1991; 11: 168–90.

Barkhof F, Scheltens P, Valk J, Waalewijn C, Uitdehaag BM, Polman CH. Serial quantitative MR assessment of optic neuritis in a case of neuromyelitis optica, using gadolinium-'enhanced' STIR imaging. Neuroradiology 1991; 33: 70–1.

Barnes D, McDonald WI, Johnson G, Tofts PS, Landon DN. Quantitative nuclear magnetic resonance imaging: characterisation of experimental cerebral oedema. J Neurol Neurosurg Psychiatry 1987; 50: 125–33.

Beck RW, Cleary PA. Optic neuritis treatment trial. One-year follow-up results. Arch Ophthalmol 1993; 111: 773–5.

Casagrande VA. A third parallel visual pathway to primate area V1. [Review]. Trends Neurosci 1994; 17: 305–10.

Dain SJ, Rammohan KW, Benes SC, King-Smith PE. Chromatic, spatial, and temporal losses of sensitivity in multiple sclerosis. Invest Ophthalmol Vis Sci 1990; 31: 548–58.

Davies MB, Williams R, Haq N, Pelosi L, Hawkins CP. MRI of optic nerve and postchiasmal visual pathways and visual evoked potentials in secondary progressive multiple sclerosis. Neuroradiology 1998, 40: 765–70.

DeYoe EA, Van Essen DC. Concurrent processing streams in monkey visual cortex. [Review]. Trends Neurosci 1988; 11: 219–26.

Efron B, Tibshirani RJ. An introduction to the bootstrap. New York: Chapman & Hall; 1993.

Fallowfield L, Krauskopf J. Selective loss of chromatic sensitivity in demyelinating disease. Invest Ophthalmol Vis Sci 1984; 25: 771–3.

Ferrera VP, Nealey TA, Maunsell JH. Mixed parvocellular and magnocellular geniculate signals in visual area V4. Nature 1992; 358: 756–61.

Filippi M, Horsfield MA, Bressi S, Martinelli V, Baratti C, Reganati P, et al. Intra- and inter-observer agreement of brain MRI lesion volume measurements in multiple sclerosis. A comparison of techniques. Brain 1995; 118: 1593–600.

Foster DH. Psychophysical loss in optic neuritis: luminance and colour aspects. In: Hess RF, Plant GT, editors. Optic neuritis. Cambridge: Cambridge University Press; 1986. p. 152–91.

Foster DH, Bischof WF. Thresholds from psychometric functions: superiority of bootstrap to incremental and probit variance estimators. Psychol Bull 1991; 109: 152–9.

Foster DH, Snelgar RS, Heron JR. Abnormal chromatic and luminance sensitivity in multiple sclerosis [abstract]. Electroencephalogr Clin Neurophysiol 1983; 56: 16P.

Foster DH, Snelgar RS, Heron JR. Nonselective losses in foveal chromatic and luminance sensitivity in multiple sclerosis. Invest Ophthalmol Vis Sci 1985; 26: 1431–41.

Gass A, Moseley IF, Barker GJ, Jones S, MacManus D, McDonald WI, et al. Lesion discrimination in optic neuritis using high-resolution fat-suppressed fast spin-echo MRI. Neuroradiology 1996; 38: 317–21.

Glynn RJ, Rosner B. Accounting for the correlation between fellow eyes in regression analysis. Arch Ophthalmol 1992; 110: 381–7.

Grimaud J, Barker GJ, Wang L, Lai M, MacManus DG, Webb SL, et al. Correlation of magnetic resonance imaging parameters with clinical disability in multiple sclerosis: a preliminary study. J Neurol 1999; 246: 961–7.

Halliday AM, McDonald WI, Mushin J. Visual evoked response in diagnosis of multiple sclerosis. Br Med J 1973; 4: 661–4.

Hawkins CP, Munro PM, MacKenzie F, Kesselring J, Tofts PS, du Boulay EP, et al. Duration and selectivity of blood–brain barrier breakdown in chronic relapsing experimental allergic

encephalomyelitis studied by gadolinium-DTPA and protein markers. Brain 1990; 113: 365–78.

Herbst H, Ketabi A, Thier P, Dichgans J. Comparison of psychophysical and evoked potential methods in the detection of visual deficits in multiple sclerosis. Electroencephalogr Clin Neurophysiol 1997; 104: 82–90.

Hornabrook RS, Miller DH, Newton MR, MacManus DG, du Boulay EP, Halliday AM, et al. Frequent involvement of the optic radiation in patients with acute isolated optic neuritis. Neurology 1992; 42: 77–9.

Ingling CR Jr, Martinez-Uriegas E. The relationship between spectral sensitivity and spatial sensitivity for the primate r-g X-channel. Vision Res 1983; 23: 1495–500.

Kapoor R, Miller DH, Jones SJ, Plant GT, Brusa A, Gass A, et al. Effects of intravenous methylprednisolone on outcome in MRI-based prognostic subgroups in acute optic neuritis. Neurology 1998; 50: 230–7.

Mason RJ, Snelgar RS, Foster DH, Heron JR, Jones RE. Abnormalities of chromatic and luminance critical flicker frequency in multiple sclerosis. Invest Ophthalmol Vis Sci 1982; 23: 246–52.

Maunsell JH, Nealey TA, DePriest DD. Magnocellular and parvocellular contributions to responses in the middle temporal visual area (MT) of the macaque monkey. J Neurosci 1990; 10: 3323–34.

Maunsell JH, Ghose GM, Assad JA, McAdams CJ, Boudreau CE, Noerager BD. Visual response latencies of magnocellular and parvocellular LGN neurons in macaque monkeys. Vis Neurosci 1999; 16: 1–14.

McDonald WI, Barnes D. The ocular manifestations of multiple sclerosis. 1. Abnormalities of the afferent visual system. [Review]. J Neurol Neurosurg Psychiatry 1992; 55: 747–52.

Merigan WH, Katz LM, Maunsell JH. The effects of parvocellular lateral geniculate lesions on the acuity and contrast sensitivity of macaque monkeys. J Neurosci 1991; 11: 994–1001.

Miller DH. The spectrum of abnormalities in multiple sclerosis. In: Muller DH, Kesselring J, McDonald WI, Paty DW, Thompson AJ, editors. Magnetic resonance in multiple sclerosis. Cambridge: Cambridge University Press; 1997. p. 31–62.

Miller DH, Rudge P, Johnson G, Kendall BE, MacManus DG, Moseley IF, et al. Serial gadolinium enhanced magnetic resonance imaging in multiple sclerosis. Brain 1988; 111: 927–39.

Miller NR, editor. Walsh and Hoyt's clinical neuro-ophthalmology. 4th edn. Baltimore: Williams and Wilkins; 1982. p. 69–86.

Mullen KT. The contrast sensitivity of human colour vision to red–green and blue–yellow chromatic gratings. J Physiol (Lond) 1985; 359: 381–400.

Mullen KT, Plant GT. Colour and luminance vision in human optic neuritis. Brain 1986; 109: 1–13.

Nealey TA, Maunsell JH. Magnocellular and parvocellular contributions to the responses of neurons in macaque striate cortex. J Neurosci 1994; 14: 2069–79.

Ormerod IE, McDonald WI, du Boulay EP, Kendall BE, Moseley IF, Halliday AM, et al. Disseminated lesions at presentation in patients with optic neuritis. J Neurol Neurosurg Psychiatry 1986; 49: 124–7.

Ormerod IE, Miller DH, McDonald WI, du Boulay EP, Rudge P, Kendall BE, et al. The role of NMR imaging in the assessment of multiple sclerosis and isolated neurological lesions. A quantitative study. Brain 1987; 110: 1579–616.

Patterson VH, Heron JR. Visual field abnormalities in multiple sclerosis. J Neurol Neurosurg Psychiatry 1980; 43: 205–9.

Perkin GD, Rose FC, editors. Optic neuritis and its differential diagnosis. Oxford: Oxford University Press; 1979.

Phillips ML, Foster DH, Honan WP, Edgar GK, Heron JR. Optic neuritis. Differential losses of luminance and chromatic function near a scotoma. Brain 1994; 117: 767–73.

Plant GT. Disorders of colour vision in diseases of the nervous system. In: Foster DH, editor. Inherited and acquired colour vision deficiencies. Vision and visual dysfunction, Vol. 7. Basingstoke (UK): Macmillan; 1991. p. 173–98.

Plant GT, Hess RF. Temporal frequency discrimination in optic neuritis and multiple sclerosis. Brain 1985; 108: 647–76.

Plant GT, Hess RF. Regional threshold contrast sensitivity within the central visual field in optic neuritis. Brain 1987; 110: 489–515.

Plant GT, Kermode AG, Turano G, Moseley IF, Miller DH, MacManus DG, et al. Symptomatic retrochiasmal lesions in multiple sclerosis: clinical features, visual evoked potentials, and magnetic resonance imaging. Neurology 1992; 42: 68–76.

Porciatti V, Sartucci F. Retinal and cortical evoked responses to chromatic contrast stimuli. Specific losses in both eyes of patients with multiple sclerosis and unilateral optic neuritis. Brain 1996; 119: 723–40.

Poser S, Wikstrom J, Bauer HJ. Clinical data and identification of special forms of multiple sclerosis in 1271 cases studied with a standardised documentation system. J Neurol Sci 1979; 40: 159–68.

Poser CM, Paty DW, Scheinberg L, McDonald WI, Davis FA, Ebers GC, et al. New diagnostic criteria for multiple sclerosis: guidelines for research protocols. Ann Neurol 1983; 13: 227–31.

Regan D, Kothe AC, Sharpe JA. Recognition of motion-defined shapes in patients with multiple sclerosis and optic neuritis. Brain 1991; 114: 1129–55.

Russell MH, Murray IJ, Metcalfe RA, Kulikowski JJ. The visual defect in multiple sclerosis and optic neuritis. A combined psychophysical and electrophysiological investigation. Brain 1991; 114: 2419–35.

Schiller PH, Logothetis NK, Charles ER. Parallel pathways in the visual system: their role in perception at isoluminance. Neuropsychologia 1991; 29: 433–41.

Shapley R. Visual sensitivity and parallel retinocortical channels. [Review]. Annu Rev Psychol 1990; 41: 635–58.

Silveira LC, Perry VH. The topography of magnocellular projecting ganglion cells (M-ganglion cells) in the primate retina. Neuroscience 1991; 40: 217–37.

Snelgar RS, Foster DH, Heron JR, Jones RE, Mason RJ. Multiple sclerosis: abnormalities in luminance, chromatic, and temporal function at multiple retinal sites. Doc Ophthalmol 1985; 60: 79–92.

Taylor MM, Creelman CD. PEST: efficient estimates on probability functions. J Acoust Soc Am 1967; 41: 782–7.

Travis D, Thompson P. Spatiotemporal contrast sensitivity and colour vision in multiple sclerosis. Brain 1989; 112: 283–303.

Ulrich J, Groebke-Lorenz W. The optic nerve in multiple sclerosis: a morphological study with retrospective clinico-pathological correlations. Neuro-ophthalmology 1983; 3: 149–59.

van Walderveen MA, Barkhof F, Hommes OR, Polman CH, Tobi H, Frequin ST, et al. Correlating MR imaging and clinical disease activity in multiple sclerosis: relevance of hypointense lesions on short TR/short-TE (T1-weighted) spin-echo images. Neurology 1995; 45: 1684–90.

van Walderveen MA, Kamphorst W, Scheltens P, van Waesberghe JH, Ravid R, Valk J, et al. Histopathologic correlate of hypointense lesions on T1-weighted spin-echo MRI in multiple sclerosis. Neurology 1998; 50: 1282–8.

Vleugels L, Van Nunen A, Lafosse C, Ketelaer P, Vandenbussche E. Temporal and spatial resolution in foveal vision of multiple sclerosis patients. Vision Res 1998; 38: 2987–97.

Wall M. Loss of P retinal ganglion cell function in resolved optic neuritis. Neurology 1990; 40: 649–53.

Youl BD, Turano G, Miller DH, Towell AD, MacManus DG, Moore SG, et al. The pathophysiology of acute optic neuritis. An association of gadolinium leakage with clinical and electrophysiological deficits. Brain 1991; 114: 2437–50.

Young IR, Hall AS, Pallis CA, Legg NJ, Bydder GM, Steiner RE. Nuclear magnetic resonance imaging of the brain in multiple sclerosis. Lancet 1981; 2: 1063–6.

Zisman F, King-Smith PE, Bhargava SK. Spectral sensitivities of acquired color defects analyzed in terms of color opponent theory. Mod Probl Ophthalmol 1978; 19: 254–7.

*Received June 3, 1999. Revised December 22, 1999.*
*Accepted February 21, 2000*